Preprints of the 19th World Congress
The International Federation of Automatic Control
Cape Town, South Africa. August 24-29, 2014

Implementation of the Sliding Mode Control with Constant and Varying Sliding Surfaces to a Hydraulically-Actuated Fin Loading System

Mehmet Uğur Özakalın*, Metin U. Salamcı, and Bülent Özkan*****

** The Scientific and Technological Research Council of Turkey,*
Defense Industry Research and Development Institute, Ankara, Turkey
(e-mail: ugur.ozakalin@tubitak.gov.tr)
***Gazi University, Engineering Faculty, Mechanical Engineering Department, Ankara, Turkey*
(e-mail: msalamci@gazi.edu.tr)
**** The Scientific and Technological Research Council of Turkey,*
Defense Industry Research and Development Institute, Ankara, Turkey
(e-mail: bulent.ozkan@tubitak.gov.tr)

Abstract: In this study, the implementation of the sliding mode control method to fin loading systems which are utilized in performance tests of control actuation systems converting the flight commands into physical motion in autonomous aerial systems is investigated. For this purpose, the mathematical model of a hydraulically-actuated fin loading system designed to accomplish the mentioned objective is built and then the sliding mode control schemes involving both constant and varying sliding surfaces are constructed. Having completed the computer simulations upon these models under specified conditions, real-time performance tests are conducted using the experimental setup developed. As a result of the simulations and experiments, it is observed that the varying-surface sliding mode control approach exceeds other control methods examined in performance.

Keywords: Fin loading system, hydraulic actuation, sliding mode control, constant sliding surface, varying sliding surface.

1. INTRODUCTION

Fin loading systems (FLSs) which are developed to generate aerodynamic loads acting on the control actuation systems (CASs) of autonomous aerial systems such as guided munitions and unmanned aerial vehicles throughout their flight to the CASs on the ground are designed in either electromechanical or hydraulic manner depending on the amplitude and duration characteristics of the loads specified (Özakalın, 2010). Under the circumstances in which the amplitude of the loads are high and the duration of the operation is relatively long, hydraulically-actuated FLSs are preferred by considering their high bandwidth and low heating properties in addition to their high loading capacity. On the other hand, since the fin angle commands which are realized by the CASs upon which the external loads are applied behave as disturbances on the FLSs, it is required that robust control methods be utilized so as to minimize the diverting effects of these disturbances whose amplitude and direction vary randomly in time on the FLSs (Nam *et al.*, 2000). In this extent, norm-based robust control schemes such as H_2 and H_∞ are proposed as well as the classical control algorithms based on PID (proportional plus integral plus derivative) and PI (proportional plus integral) control actions (Özakalın *et al.*, 2010).

In this study, the sliding mode control method which constitutes one of the robust control approaches is implemented on a hydraulically-actuated FLS considered. For this purpose, a classical control system based on the PID action is build in order to generate the hinge moment effect resulted from the aerodynamic loads on the fin connecting rod at the first attempt and then the sliding mode control algorithms are designed with constant and varying sliding surfaces (Bandyopadhyay *et al.*, 2009, Park, 2000, and Piltan *et al.*, 2011). The mentioned variation on the sliding surfaces is accomplished in two different ways: a linear form in time and fuzzy logic-based (Tokat *et al.*, 2009 and Gökbilen, 2006). Here, in order to remove or at least minimize the chattering effect originating from the nonlinear characteristic of the signum function used in the command signal of the sliding mode control, the saturation function and fuzzy transition function are considered. When these functions are designated, it is accounted to relinquish from the stability as minimum as possible in addition to diminishing the chattering effect. Having completed the computer simulations for all the control system algorithms established, the real-time experiments are conducted using the test setup developed. Thus, it is seen that the sliding mode control system with a varying sliding surface yields the most satisfactory results.

2. DYNAMIC MODELING OF THE FIN LOADING SYSTEM

The schematical representation of the considered FLS combined of four identical hydraulic actuation units is shown in Fig. 1 where p_1 and p_2 denote the pressure values of the hydraulic fluid in the inlet and outlet ports of the hydraulic cylinder, and p_S and p_R represent the pressure values of the

hydraulic fluid in the inlet of the fluid control valve and return line to the hydraulic fluid tank, respectively.

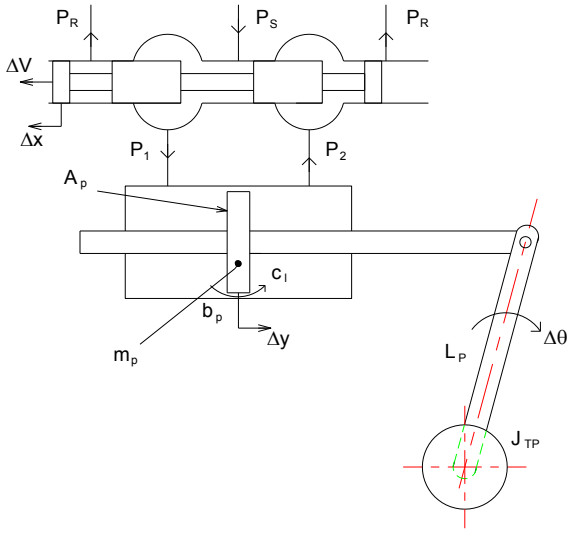

Fig. 1. View of the hydraulically-actuated fin loading system.

The dynamics of the servovalve as the flow control valve can be expressed by the forthcoming first-order transfer function:

$$\frac{\Delta x}{\Delta I} = \frac{K_v}{T_v\, s + 1} \tag{1}$$

where Δx, ΔI, K_v, and T_v denote the displacement of the servovalve control spool, control current to the servovalve, gain, and time constant of the valve, respectively. In modeling, the servovalve dynamics is ignored for the sake of simplifying the design process and thus it is assumed that the transfer function given in equation (1) is approximated by K_v

The equation between the displacement of the valve control spool and load pressure can be expressed as

$$\Delta Q_L = c_x\, \Delta x - c_p\, \Delta p_L \tag{2}$$

where ΔQ_L, Δp_L, c_x, and c_p are the volumetric flow rate, load pressure, valve gain and valve pressure coefficient.

In equation (2), Δp_L is defined as the difference between the pressures of the valve chambers, i.e. p_1 and p_2 as follows:

$$\Delta p_L = p_1 - p_2 \tag{3}$$

The flow rate from the valve to the hydraulic cylinder is

$$\Delta Q_L = A_p\, \Delta \dot{y} + \left[V/(2\beta)\right] \Delta \dot{p}_L + c_l\, \Delta p_L \tag{4}$$

where A_p, V, β, c_l, $\Delta \dot{y}$, Δp_L, and $\Delta \dot{p}_L$ correspond to the cross-sectional area of the piston in the hydraulic cylinder perpendicular to the flow, volume of each of the two chambers divided by the piston inside the hydraulic cylinder, Bulk modulus, fluid leakage coefficient, linear velocity of the piston of the hydraulic cylinder along the motion axis, load pressure, and time derivative of the load pressure.

Matching equations (2) and (4) yields the next equality:

$$\left[V/(2\beta)\right] \Delta \dot{p}_L + \left(c_l + c_p\right) \Delta p_L + A_p\, \Delta \dot{y} = c_x\, \Delta x \tag{5}$$

The piston dynamic can be expressed as follows:

$$m_p\, \Delta \ddot{y} + b_p\, \Delta \dot{y} + \Delta F_p = A_p\, \Delta p_L \tag{6}$$

where m_p, b_p, ΔF_p and $\Delta \ddot{y}$ stand for the piston mass, viscous friction coefficient between the piston and cylinder, force applied by piston to the fin and acceleration of the piston respectively.

Using equation (6), Δp_L and its first time derivative are obtained in the following manner:

$$\Delta p_L = \left(m_p\, \Delta \ddot{y} + b_p\, \Delta \dot{y} + \Delta F_p\right)/A_p \tag{7}$$

$$\Delta \dot{p}_L = \left(m_p\, \Delta \dddot{y} + b_p\, \Delta \ddot{y} + \Delta \dot{F}_p\right)/A_p \tag{8}$$

As J_{Tp} represents the mass moment of inertia of the half portion of the torquemeter put between the fin connecting rod and transmission rod to measure the amount of the torque applied on the fin connecting rod around the rotation axis of the fin connecting rod, ΔF_p and its first time derivative can be determined as follows:

$$\Delta F_p = J_{Tp}\, \Delta \ddot{\theta} \tag{9}$$

$$\Delta \dot{F}_p = J_{Tp}\, \Delta \dddot{\theta} \tag{10}$$

The relationship between the angular displacement of the fin and linear displacement of the piston can be established from Fig. 1 along with its successive time derivatives using the small angle assumption in the following manner:

$$\Delta y = L_p\, \Delta \theta \tag{11}$$

$$\Delta \dot{y} = L_p\, \Delta \dot{\theta} \tag{12}$$

$$\Delta \ddot{y} = L_p\, \Delta \ddot{\theta} \tag{13}$$

$$\Delta \dddot{y} = L_p\, \Delta \dddot{\theta} \tag{14}$$

Substituting equations (9) through (14) into equations (7) and (8) give the forthcoming expressions:

$$\Delta p_L = \left[\left(J_{Tp} + m_p\, L_p\right)\Delta \ddot{\theta} + b_p\, L_p\, \Delta \dot{\theta}\right]/A_p \tag{15}$$

$$\Delta \dot{p}_L = \left[\left(J_{Tp} + m_p\, L_p\right)\Delta \dddot{\theta} + b_p\, L_p\, \Delta \ddot{\theta}\right]/A_p \tag{16}$$

Inserting equations (12), (15), and (16) into equation (5) and arranging it, the differential equation describing the dynamic behaviour of the hydraulic FLS can be derived in the following manner (Özakalın, 2010 and Özakalın *et al.*, 2010):

$$d_3\, \Delta \dddot{\theta} + d_2\, \Delta \ddot{\theta} + d_1\, \Delta \dot{\theta} = c_x\, \Delta x \tag{17}$$

In the equation above, as $d_1 = \left[\left(c_l + c_p\right) b_p\, L_p^2 / A_p\right] + A_p\, L_p^2$

$d_2 = \left[\left(V\, b_p\, L_p^2\right)/\left(2\beta\, A_p\right)\right] + \left(c_l + c_p\right)\left(J_{Tp} + m_p\, L_p^2\right)/A_p$, and

$d_3 = V\left(J_{Tp} + m_p\, L_p^2\right)/\left(2\beta\, A_p\right)$

Also in those equations, the small displacements of the system from the equilibrium conditions are symbolized by Δ.

Applying the Laplace transformation to equation (17) after simplifying it, the transfer function between the linear displacement of the valve control spool (Δx) and angular displacement of the transmission rod ($\Delta\theta$) is obtained as in equation (18):

$$\frac{\Delta\theta(s)}{\Delta X(s)} = \frac{c_x}{d_3\, s^3 + d_2\, s^2 + d_1\, s} \tag{18}$$

Since the control variable of the considered system and output signal of the controller are the torque quantity on the fin connecting rod (ΔT) and control voltage of the valve (ΔV), respectively, regarding the relationship in equation (1) as well, the transfer function between ΔV and ΔT is found by multiplying the transfer function in equation (18) with the torquemeter constant (K_s) as follows:

$$\frac{\Delta T(s)}{\Delta V(s)} = \frac{K_v K_s c_x}{d_3 s^3 + d_2 s^2 + d_1 s} \tag{19}$$

Transfer function in equation (19) can be modified with the definition of the electrical charge quantity (ΔQ) as

$$\frac{\Delta T(s)}{\Delta V(s)/s} = \frac{K_v K_s c_x}{d_3 s^2 + d_2 s + d_1} \tag{20}$$

$$\Delta V(s)/s = \Delta Q(s) \tag{21}$$

Eventually, putting equation (21) into equation (20) produces the transfer function between ΔQ and ΔT as given below:

$$\frac{\Delta T(s)}{\Delta Q(s)} = \frac{K_v K_s c_x}{d_3 s^2 + d_2 s + d_1} \tag{22}$$

3. CONTROL SYSTEM DESIGN FOR THE FIN LOADING SYSTEM

In the scope of this study, three different control systems are designed in order for the FLS to produce the specified hinge moment quantities on the fin connecting rod at a desired accuracy level:

i. Classical control system based on the PID action,

ii. Sliding mode control system with a constant sliding surface,

iii. Sliding mode control system with a varying sliding surface.

3.1 Classical Control System based on the PID Action

When the relevant previous studies are examined, it is observed that the third time derivative of the torque variable which is multiplied by the Bulk modulus as well does not affect the system response significantly. Thus, ignoring the servovalve dynamics for simplifying the controller design process and reducing the order of the system to two by disregarding the effect of the Bulk modulus, i.e. by skipping the term multiplied with the third order time derivative of the torque, for simplifying the controller design, the transfer function of the classical torque control system for which the hinge moment is selected as the control variable is determined according to the PID action by regarding the equation of motion in equation (17) as ΔT_d indicates the desired, i.e. reference, value of the hinge moment in the following fashion (Özakalın *et al.*, 2010):

$$\frac{\Delta T(s)}{\Delta T_d(s)} = \frac{G_o(s)}{1+G_o(s)} = \frac{N(s)}{D(s)} \tag{23}$$

As K_p, K_i, and K_d denote the proportional, integral, and derivative gains of the controller, respectively, the following definitions are introduced in equation (23):

$$G_o(s) = \frac{K_v K_s c_x \left[K_p + (K_i/s) + K_d s\right]}{d_2 s^2 + d_1 s} \tag{24}$$

$$N(s) = \left(K_p s + K_i + K_d s^2\right) K_v K_s c_x \tag{25}$$

$$D(s) = d_2 s^3 + \left(d_1 + K_v K_s K_d c_x\right)s^2 + \left(K_v K_s K_p c_x\right)s + K_v K_s K_i c_x \tag{26}$$

The gains of the third order control system whose characteristic polynomial appears as in equation (26) can be designated by the pole placement in the complex plane so as to satisfy the predefined performance specifications. Hence, these gains are calculated by equating polynomial *D(s)* to the characteristic polynomial of the ideal third order control system [$D_3(s)$] as given below as a function of the desired bandwidth (ω_c) and damping ratio (ζ_c) parameters of the control system (Özakalın *et al.*, 2010):

$$D_3(s) = \left(\frac{1}{\omega_c^3}\right)s^3 + \left(\frac{2\zeta_c + 1}{\omega_c^2}\right)s^2 + \left(\frac{2\zeta_c + 1}{\omega_c}\right)s + 1 \tag{27}$$

Equating equations (26) and (27) to each other, the controller gains come into the picture in the following manner:

$$K_p = \left[(2\zeta_c + 1)d_2 \omega_c^2\right]/(K_v K_s c_x) \tag{28}$$

$$K_i = \left(d_2 \omega_c^3\right)/(K_v K_s c_x) \tag{29}$$

$$K_d = \left[(2\zeta_c + 1)d_2 \omega_c - d_1\right]/(K_v K_s c_x) \tag{30}$$

3.2 Sliding Mode Control System with a Constant Sliding Surface

Choosing variables ΔT and $\Delta \dot{T}$ as the first and second state variables for the plant under consideration, that is, defining $x_1 = \Delta T$ and $x_2 = \dot{x}_1 = \Delta \dot{T}$ and assigning the system input to be $u=\Delta I$, the plant dynamics can be written in the state-space form with the use of equation (17) in the following manner:

$$\dot{x}_1 = x_2 \tag{31}$$

$$\dot{x}_2 = -(d_1/d_2)x_2 + K_v K_s c_x u \tag{32}$$

Rearranging equations (31) and (32) by introducing the system output as $y=\Delta T$, the error dynamics of the system can be formed as regarding the error parameter to be $e = \Delta T_d - \Delta T$ as follows:

$$\ddot{e} = \ddot{x}_{1d} - \ddot{x}_1 = \ddot{x}_{1d} - \dot{x}_2 = \ddot{x}_{1d} + \frac{d_1}{d_2}x_2 - \frac{K_v K_s c_x}{d_2}u \tag{33}$$

The switching function for the sliding function (s) is designated as given below with λ denotes the slope of "s":

$$s = \dot{e} + \lambda e \tag{34}$$

The Lyapunov function selected in the following manner can be used to guarantee the stability of the sliding mode control system to be designed:

$$V(s) = (1/2)s^2 \tag{35}$$

In order for the sliding mode control system to be stable, the conditions $V(s)>0$ and $\dot{V}(s)<0$ should be satisfied for $s>0$

as well as *V(0)=0*. While the first and third conditions are directly satisfied by equation (35), the second condition leads the control law which will be valid for the sliding mode control system to be determined as follows:

$$u = \frac{d_2}{K_v K_s c_x}\left[\mu sgn(s) + \ddot{x}_{1d} + \frac{d_1}{d_2}x_2 + \lambda\left(\dot{x}_{1d} - x_2\right)\right] \quad (36)$$

where the term sgn(·) shows the signum function with μ stands for the positive control gain and $x_{1d}=\Delta T_d$.

Also, as t_s and s_0 indicate the reaching time to the sliding surface and value of the sliding function defined in equation (19) at the beginning of the control process, the parameters λ and μ can be calculated from the next formulas:

$$\lambda = \omega_c \quad (37)$$

$$\mu = s_0 / t_s \quad (38)$$

3.3 Sliding Mode Control System with a Varying Sliding Surface

In the sliding mode control method, the control law yields a control signal whose amplitude and direction alter continuously to maintain the stability of the system throughout a planned operation. This causes the phenomenon called chattering. In order to remove this unfavourable situation, the use of the sliding mode control with a varying sliding surface is one of the proposed approaches (Tokat *et al.*, 2009). In this manner, the sliding surface varies in accordance with the system response while trying to keep the stability of the system and thus the chattering is diminished.

In the sliding mode control system with the varying sliding surface, λ and β are defined at the initiation of the process with the forthcoming linear functions as *t* indicates the time variable:

$$\lambda = \lambda(t) = \lambda_1 t + \lambda_0 \quad (39)$$

$$\beta = \beta(t) = \beta_1 t + \beta_0 \quad (40)$$

Deciding on the coefficients λ_0, λ_1, β_0, and β_1 in equations (39) and (40), as per the definitions of the regions on the error (*e*) vs. error rate ($\dot{e}$) plane given in Fig. 2, the situations listed below are taken into account (Bartoszewicz, 2007):

i. Sliding surface has only rotation in regions II and IV which are called "stable regions" but no translation. Therefore, $\beta(t) = 0$.

ii. Sliding surface has only translation in regions I and III which are called "unstable regions" but no rotation. This condition leads $\lambda(t) = \lambda_0$ (constant).

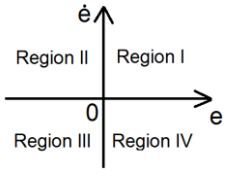

Fig. 2. Regions on the error-error rate plane

Considering the conditions given above, the control law is obtained for the sliding mode control system with the varying sliding surface as follows:

$$u = \frac{x_2\left(d_1 - \lambda d_2\right) + d_2\left[\mu sgn(s) + \beta_1 + x_{1d}\lambda_1 + \dot{x}_{1d}\lambda + \ddot{x}_{1d}\right]}{K_v K_s c_x} \quad (41)$$

In the second control algorithm with a varying sliding surface, parameters λ and β are specified by means of the fuzzy logic-based triangular membership functions unlike the preceding linear approach. In this second case, the control law formulated in equation (41) is used, too (Özakalın, 2010).

4. COMPUTER SIMULATIONS AND TESTS

In order for the control systems whose mathematical models are developed as explained above to be realized, the test setup consisting of a hydraulic actuator used as the actuator, speed reducer, and torquemeter is given in Fig. 3.

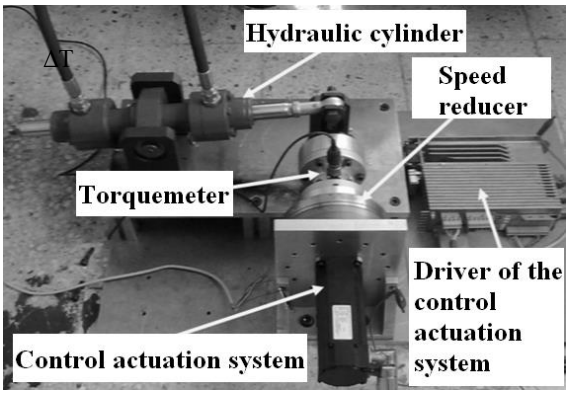

Fig. 3. Test setup for the hydraulically-actuated fin loading system (Özakalın, 2010).

Table 1. Numerical values used in the simulations

Parameter	Numerical Value
J_{Tp}	2.04x10^{-3} kg·m^2
m_p	5 kg
b_p	400 N·s/m
V	0.747x10^{-4} m^3
A_p	0.641x10^{-3} m^2
L_p	0.1 m
β	7x10^8 N/m^2
c_x	0.667 m^2/s
c_p	1.587x10^{-11} m^3/Pa
c_l	8.11x10^{-13} m^3/Pa·s
K_v	5×10^{-5} m/V
T_v	0.004 s

Having performed the system identification works using the test setup shown in Fig. 2, the natural frequency and damping ratio values of the FLS whose dynamic behavior is described as in equation (22) are calculated to be 7.071 Hz and 0.349, respectively. The numerical values of the system parameters are determined as submitted in Table 1 so as to be used in computer simulations. Furthermore, the bandwidth (ω_c) and damping ratio (ζ_c) parameters of the control system are considered to be 62.83 rad/s (=10 Hz) and 0.7, respectively.

In the real-time computer simulations and tests, the electrical current capacity of the driver of the CAS, sampling frequency of the control system, and duration of the computer simulations are chosen as 8 A, 2000 Hz, and 1 s, respectively (Özakalın, 2010). Here, since the expected settling time value as per the designated bandwidth quantity becomes smaller than 200 ms, the simulation duration is selected to be 1 s in order to increase the resolution of the results.

In the end of the computer simulations carried out in the MATLAB® SIMULINK® environment and the tests conducted on the setup seen in Fig. 3., the settling time, average input (control) voltage of the servovalve, maximum overshoot, and steady state error values are presented in Table 2 and Table 3 versus the step input with the amplitude of 10° as the abbreviation SMC stand for the sliding mode control regarding all the PID-type control, sliding mode control with a constant sliding surface, sliding mode control with a linearly-varying sliding surface, and sliding mode control with a fuzzy logic-based varying sliding surface approaches such that they include all kinds of switching functions, namely the signum, hyperbolic, and fuzzy logic-based switching functions. The responses of the sample control systems are acquired as given in Fig. 4, Fig. 5, Fig. 8, and Fig. 10, respectively where the signum function is taken as the switching function. The input voltage of the servovalve and the changes of the sliding surfaces are also submitted in Fig. 6, Fig. 7, and Fig. 9. The mentioned plots include both the simulations and tests as letters S and T denote the simulation and the test, respectively. Also, A and D indicate the actual and desired sliding surfaces, respectively.

Table 2. Results of the computer simulations

Controller	Switching Function	Settling Time (s)	Average Input Voltage of the Valve (V)	Maximum Overshoot (N·m)	Steady State Error (N·m)
PID		0.200	2.799	2.420	$3.6\text{x}10^{-5}$
SMC with a Constant Sliding Surface	Signum	0.190	2.094	0.001	0.062
	Hyperbolic	0.150	2.022	0	$4\text{x}10^{-5}$
	Fuzzy-Logic	0.160	1.467	0	0.021
SMC with a Linearly-Varying Sliding Surface	Signum	0.130	1.853	0	0.005
	Hyperbolic	0.140	1.745	0	$1\text{x}10^{-4}$
	Fuzzy-Logic	0.150	1.064	0	0.002
SMC with a Fuzzy-Based Varying Sliding Surface	Signum	0.085	2.030	0	0.008
	Hyperbolic	0.088	3.072	0	0.021
	Fuzzy-Logic	0.092	2.262	0	0.046

Table 3. Results of the tests

Controller	Switching Function	Settling Time (s)	Average Input Voltage of the Valve (V)	Maximum Overshoot (N·m)	Steady State Error (N·m)
PID		0.200	2.799	2.380	0.015
SMC with a Constant Sliding Surface	Signum	0.190	2.248	0.001	0.008
	Hyperbolic	0.153	2.154	0.040	0.003
	Fuzzy-Logic	0.160	1.990	0	0.001
SMC with a Linearly-Varying Sliding Surface	Signum	0.140	2.139	0.050	0.041
	Hyperbolic	0.132	2.098	0.020	0.002
	Fuzzy-Logic	0.445	2.071	0.620	0.031
SMC with a Fuzzy-Based Varying Sliding Surface	Signum	0.460	2.051	0	0.152
	Hyperbolic	0.260	2.104	0	0.193
	Fuzzy-Logic	0.830	2.066	0	0.236

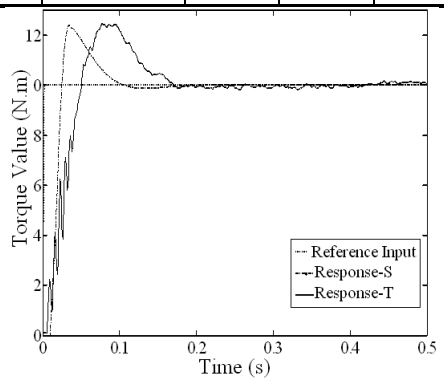

Fig. 4. Response of the PID-type control system.

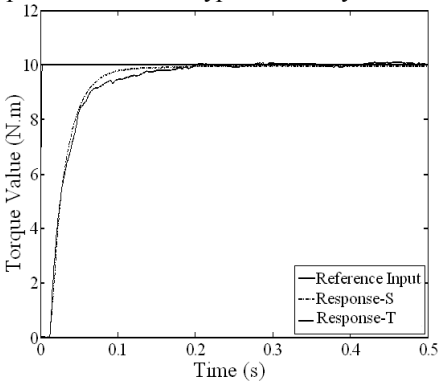

Fig. 5. Response of the sliding mode control system with a constant sliding surface.

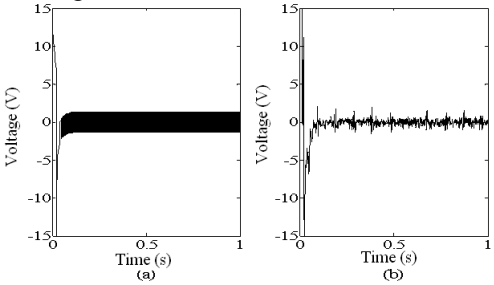

Fig. 6. Output voltage of the servovalve for SMC system with a constant sliding surface, (a) simulation and (b) test.

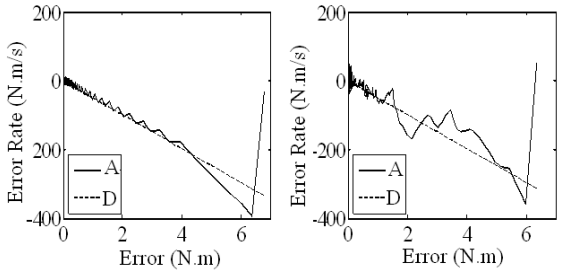

Fig. 7. Change of the sliding surface for the SMC system with the constant sliding surface, (a) simulation and (b) test.

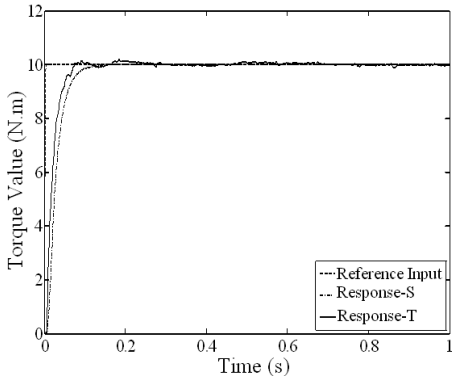

Fig. 8. Response of the sliding mode control system with the linearly-varying sliding surface.

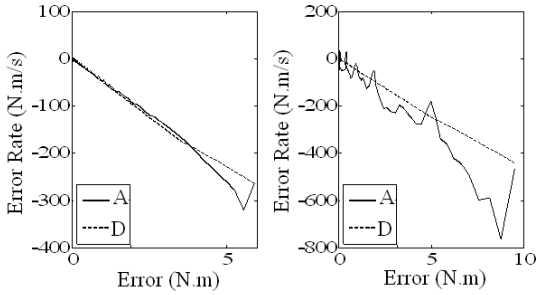

Fig. 9. Change of the sliding surface for the SMC system with the linearly-varying sliding surface, (a) simulation and (b) test.

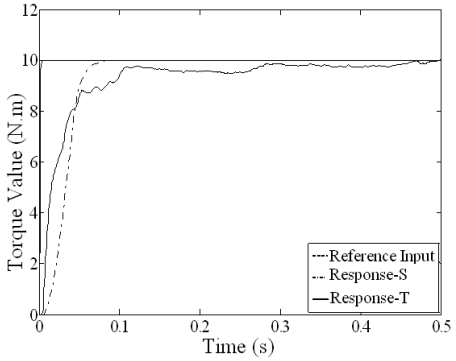

Fig. 10. Response of the sliding mode control system with the fuzzy logic-based sliding surface.

5. DISCUSSION AND CONCLUSION

When the sliding mode control systems are evaluated in overall, it is resulted that the settling time, average input voltage of the valve, maximum overshoot, and steady state error quantities attained with the use of the hyperbolic switching function are smaller compared to the signum- and fuzzy-logic-type switching functions and the worst steady state error values are encountered with the fuzzy-based-varying sliding surface. In general, the results of sliding mode control variants in this study are superior to the PID-type control except the steady state error.

In fact, the test results differ from the simulation data especially for the cases in which the sliding mode control with the fuzzy-based-varying sliding surface and the experimental measurements of the input voltage of the servovalve get lower than the simulation outputs. This is because the order of the system model used in the simulations is reduced two while the exact order order of the system is three. Also, the differences between the exact and theoretical values of the parameters contributes to these slight mismatch.

As a result, it can be concluded that the sliding mode control system with the linearly-varying sliding surface can be more implementable than its alternative with the fuzzy-based-varying-sliding surface in the physical world.

REFERENCES

Bandyopadhyay, B., Deepak, F., and Kim, K. S. (2009), *Sliding Mode Control Using Novel Sliding Surfaces*, Vol. 392, Springer.

Bartoszewicz, A. (2007), *Variable Structure Control from Principles to Applications,* Institute of Automatic Control, Technical University of Łódź, Poland.

Gökbilen, B. (2006), *Sliding Mode Control of Nonlinear Systems Using a Time-Varying Linear Surface and Applications*, MSc Thesis, Gazi University, Ankara, Turkey.

Nam, Y., Lee, J., and Sung, K. H. (2000), Force Control System Design for Aerodynamic Load Simulator, *Proceedings of the American Control Conference*, Chicago, Illinois, USA.

Özakalın, M. U. (2010), *Robust Torque Control of a Hydraulically Actuated Fin Loading System (in Turkish)*, MSc Thesis, Gazi University, Ankara, Turkey.

Özakalın, M. U., Salamcı, M. U., and Özkan, B. (2010), Control of a Hydraulically-Actuated Fin Loading System Using a Sliding Mode Controller (in Turkish), *Automatic Control Turkish National Committee, Automatic Control National Meeting-2010 (TOK'10)*, Gebze High Technology Institute, Kocaeli, Turkey.

Park, K. B. (2000), Discrete-Time Sliding Mode Controller for Linear Time-Varying Systems with Disturbances, *Transactions on Control, Automation and Systems Engineering*, Vol. 12, pp. 244-247.

Piltan, F., Sulaiman, N., Soltani, S., Marhaban, M. H., and Ramli, R. (2011), An Adaptive Sliding Surface Slope Adjustment in PD Sliding Mode Fuzzy Control for Robot Manipulator, *International Journal of Control and Automation*, Vol. 4, No. 3, pp. 65-76.

Tokat, S., Eksin, İ., and Güzelkaya, M. (2009), Linear Time Varying Sliding Surface Design Based on Co-ordinate Transformation for High-Order Systems, *Transactions of the Institute of Measurement and Control*, Vol. 31, pp. 51–70.